

A Refraction Seismic Transect from Greenland to Ellesmere Island, Canada: The Crustal Structure in Southern Nares Strait

by Thomas Funck^{1*}, H. Ruth Jackson², Sonya A. Dehler² and Ian D. Reid³

Abstract: A refraction and wide-angle reflection seismic study was carried out in southern Nares Strait (northernmost Baffin Bay) on a 378 km long profile running from Pituffik/Thule Air Base on Greenland into Makinson Inlet on Ellesmere Island, Canada. Eight ocean bottom seismometers and eight land stations were deployed to record the airgun shots along the line. A crustal velocity model was developed by forward and inverse modeling techniques. The Proterozoic Thule Basin can be correlated across Nares Strait as a continuous structure with a total thickness of 4–5 km. The basin is divided into three units. The upper unit has velocities of 4.5–5.0 km s⁻¹ and a Poisson's ratio (σ) of 0.30, indicating a high content of carbonates. The middle unit is characterized by high velocities (6.1 km s⁻¹) and a Poisson's ratio of 0.28. This unit is interpreted to correlate with the basaltic sills found in the Cape Combermere formation. The lower unit is a low-velocity zone and, hence, its velocities are unconstrained. The underlying crust is divided into three layers, upper crust (6.0–6.2 km s⁻¹, $\sigma = 0.25$), middle crust (6.1–6.3 km s⁻¹, $\sigma = 0.26$) and lower crust (6.7–6.9 km s⁻¹, $\sigma = 0.26$). These properties are consistent with a granitic/gneissic composition in the upper/middle crust and with granulites in the lower crust. Moho depth on either side of Nares Strait is 36 km, with some shallowing to 33 km in a 100 km wide zone. The Moho shallowing is related to local uplift at the Carey Islands just to the south of the line based on correlation with the gravity data. With only minor lateral changes of crustal velocities and Moho depth across southern Nares Strait, the eastern Archean/Proterozoic part of Ellesmere Island appears to be part of the same plate as Greenland with Thule Basin as intracratonic feature. No structures consistent with a strike-slip boundary could be resolved in southern Nares Strait.

Zusammenfassung: In der südlichen Nares-Strait (nördlichste Baffin Bay) wurde eine refraktionsseismische und weitwinkel-reflexionsseismische Vermessung entlang eines 378 km langen Profils durchgeführt, das von Pituffik/Thule Air Base in Grönland nach Makinson Inlet auf Ellesmere Island in Kanada verläuft. Entlang des Profils wurden acht Ozeanbodenseismometer und acht Landstationen ausgebracht, um die Airgun-Schüsse zu registrieren. Mithilfe von Vorwärtsmodellierung und Inversion wurde ein Geschwindigkeitsmodell für die Kruste entwickelt. Das proterozoische Thule Basin kann als kontinuierliche Struktur durch die Nares-Strait korreliert werden und hat eine Gesamtmächtigkeit von 4–5 km. Das Becken ist in drei Einheiten untergliedert. Die oberste Einheit hat Geschwindigkeiten zwischen 4.5–5.0 km s⁻¹ und eine Poissonzahl (σ) von 0.30, was auf einen hohen Kohlenstoffgehalt hindeutet. Die mittlere Einheit ist durch hohe Geschwindigkeiten (6.1 km s⁻¹) und eine Poissonzahl von 0.28 gekennzeichnet. Die Interpretation dieser Einheit führt zu einer Korrelation mit den basaltischen Sills der Cape Combermere Formation. Die untere Einheit ist eine Zone erniedrigter Geschwindigkeiten, weswegen ihr genauerer Wert nicht ermittelt werden konnte. Die darunterliegende Kruste ist in drei Bereiche untergliedert: Obere (6.0–6.2 km s⁻¹, $\sigma = 0.25$), mittlere (6.1–6.3 km s⁻¹, $\sigma = 0.26$) und untere Kruste (6.7–6.9 km s⁻¹, $\sigma = 0.26$). Diese Werte sind im Einklang mit einer granit- und gneisshaltigen Zusammensetzung der oberen und mittleren Kruste sowie mit Granulit in der Unterkruste. Zu beiden Seiten der Nares-Strait ist die Mohotiefe 36 km. Nur in einer 100-kmweiten Zone nimmt sie eine geringere Tiefe von 33 km ein. Die Korrelation mit Schweredaten ergibt, dass die Verringerung der Mohotiefe in Zusammenhang mit lokaler Hebung der Carey Inseln

steht, die sich unmittelbar südlich des Profils befinden. Aufgrund der nur geringen Änderungen der Krustengeschwindigkeiten und der Mohotiefe entlang der Nares Strait erscheint der östliche archaische/proterozoische Teil von Ellesmere Island als Teil der Grönländischen Platte mit dem Thule Basin als interktonische Struktur. Es konnten keine Strukturen aufgelöst werden, die für eine Blattverschiebung in der südlichen Nares Strait sprechen würden.

INTRODUCTION

The Nares Strait controversy as discussed in DAWES & KERR (1982a) concerns whether or not the strait is the plate boundary between Greenland and North America, and how much strike-slip movement occurred along this boundary. DAWES & KERR (1982b) argue that there is little or no strike-slip displacement along Nares Strait, on the basis of present-day continuity of geological features from Ellesmere Island, Canada, to Greenland. However, based on plate tectonic reconstructions, SRIVASTAVA (1985) suggests that Greenland moved 150 km northwards relative to North America, most of which should have been taken up by sinistral strike-slip movement in Nares Strait. Hence, there is an apparent incompatibility between the onshore geology surrounding Nares Strait and plate tectonic models describing the opening of the North Atlantic and the resulting motions of Greenland.

It is clear that the controversy can only be resolved by detailed mapping of the strait itself to find evidence for one model or the other. Therefore a multidisciplinary experiment was carried out in August–September 2001, including geological field work onshore and regional geophysical measurements to extend the interpretations offshore. The survey also comprised three refraction/wide-angle reflection seismic lines (FUNCK et al. 2002) with Line 3 in southern Nares Strait (Fig. 1) being the focus of this paper. The objective of the transect was to determine the crustal velocity structure across Nares Strait and to interpret the structure in terms of the tectonic evolution of Nares Strait. Earlier refraction seismic data just to the south of Line 3 (Fig. 1) give some indication for a plate boundary (JACKSON & REID 1994, REID & JACKSON 1997). However, these earlier lines are also affected by rift-related crustal thinning in northern Baffin Bay. Our Line 3 farther to the north is expected to be less influenced by this additional complexity.

GEOLOGICAL SETTING

In northern Baffin Bay onshore of refraction Line 3, two rock types predominate (Fig. 1). The exposures are either Archean and lower Proterozoic metamorphic to plutonic basement rocks or the slightly deformed and almost unmetamorphosed

¹ Danish Lithosphere Centre, Øster Voldgade 10 L, 1350 Copenhagen K, Denmark.

* Now at: Geological Survey of Denmark and Greenland, Øster Voldgade 10, 1350 Copenhagen K, Denmark.

² Research Scientist, Geological Survey of Canada (Atlantic), Bedford Institute of Oceanography, P.O. Box 1006, Dartmouth, Nova Scotia, B2Y 4A2, Canada.

³ Geological Institute, University of Copenhagen, Øster Voldgade 10, DK-1350 Copenhagen K, Denmark.

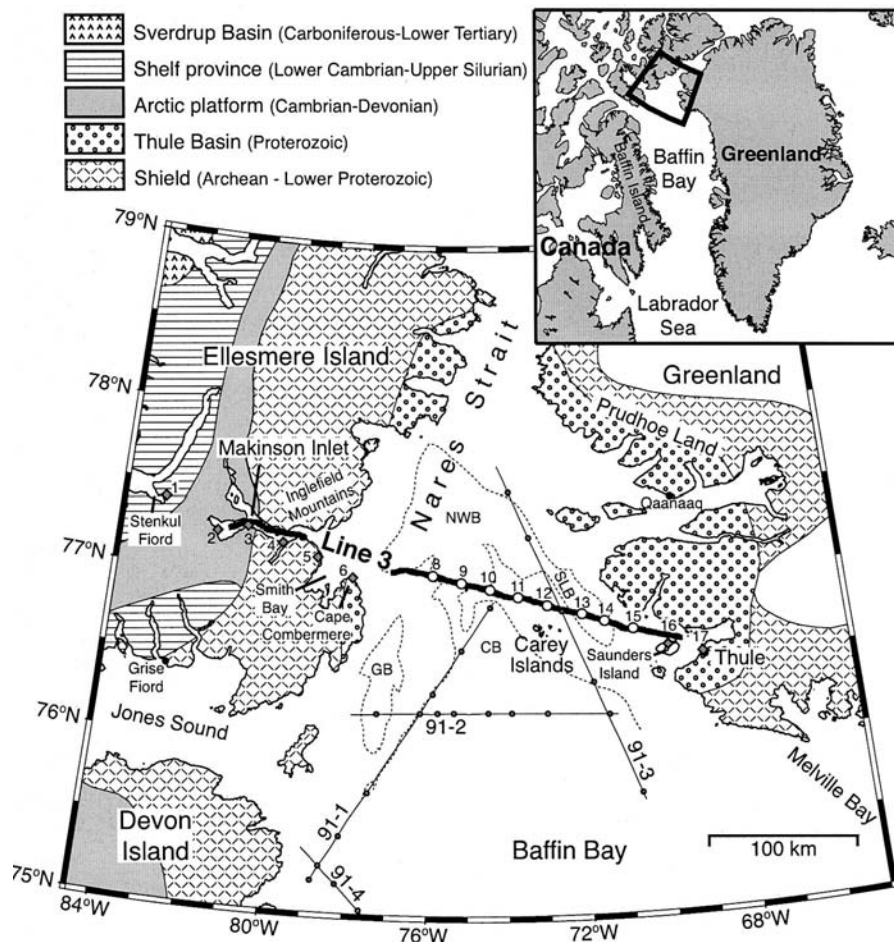


Fig. 1: Regional geology map of the study area (modified from WILLIAMSON 1988, Thule Basin taken from PEEL & CHRISTIE 1982). Dashed lines show the outline of Tertiary offshore basins (HARRISON in press). Segments with airgun shots along Line 3 are shown as bold line. Ocean bottom seismometers (OBS) are indicated by open circles and locations of land seismometers are shown as grey diamonds, annotations specify the station number. Refraction seismic lines relevant to this study are shown by thin lines with circles indicating the OBS locations: lines 91-1 and 91-3 (JACKSON & REID 1994), lines 91-2 and 91-4 (Reid & Jackson 1997). CB = Carey Basin; NWB = North Water Basin; GB = Glacier Basin; SLB = Steensby Land Basin.

rocks of the Thule Supergroup (DAWES 1997).

The Carey Islands are located just to the south of Line 3, and therefore, are particularly relevant to the geological discussion. On the islands gneiss, schists and granites are observed typical of the basement terrain on Greenland from Melville Bay north to Prudhoe Land (76°30' N – 78°30' N) (DAWES 1976). The Precambrian rocks are intruded by dolerite dykes and sills. No sedimentary rocks have been mapped (BENDIX-ALMGREEN et al. 1976).

The Thule Supergroup consists of continental to shallow marine sedimentary rocks and one main unit of basaltic volcanic rocks (DAWES 1997). Onshore it extends over 300 km from north to south (DAWES 1997). The coastal outcrops disappear under the sea in down-faulted blocks. This suggests that the onshore outcrops are the preserved fragments of a larger offshore basin. Potential field and seismic reflection profiles have been interpreted as consistent with a sedimentary section of several km thickness (KEEN & BARRETT 1973, HOOD & BOWER 1973, ROSS & FALCONER 1975, NEWMAN 1982, JACKSON et al. 1992). However, the age of the offshore sedimentary deposits is unknown.

The lack of deformation and low metamorphic grade of the Thule Supergroup suggests that little tectonic activity occurred in the region during the Phanerozoic. To the south of the study area localized deposits of younger rocks are exposed on Bylot Island. Here sedimentary deposits of Late Cretaceous to Tertiary age are mapped.

The tectonic history of northern Baffin Bay from Cretaceous to Tertiary is deduced from plate reconstructions based on regional magnetic anomalies in the Labrador Sea, Norwegian and Greenland seas and the Arctic Ocean. Local evidence of oceanic crust to the south of 76 °N based on refraction results and gravity modelling has been reported by REID & JACKSON (1997). The plate reconstructions (e.g., SRIVASTAVA 1985) and other geophysical data are consistent with an extinct spreading centre in the Labrador Sea that is postulated to continue into Baffin Bay, on the basis of a linear gravity low. The oceanic crust terminates in northern Baffin Bay. From northern Baffin Bay through Nares Strait, a plate boundary has been interpreted that is strike-slip evolving in time to a compressional zone. The plate boundary is required for Greenland to move as an independent plate. The timing of the motion and the consequence of it are consistent with the Eurekan Orogeny on Ellesmere Island and Axel Heiberg Island to the north. However, the presence of the Thule Basin, an intracratonic feature, straddling the plate boundary argues against such a dynamic history (DAWES 1976).

The rocks exposed along Nares Strait and northern Baffin Bay (TRETTIN 1991) can be divided into five types: 1) Archean to Lower Proterozoic metamorphic-plutonic basement, 2) upper Middle to Upper Proterozoic sedimentary and volcanic rocks of the Thule Supergroup, 3) undeformed Cambrian to Devonian rocks of the interior platform, 4) Lower Paleozoic rocks of the Franklinian Mobile Belt and 5) late Cretaceous and Tertiary sedimentary rocks.

WIDE-ANGLE SEISMIC EXPERIMENT

Data acquisition

The survey was carried out in August and September 2001 onboard the Canadian Coast Guard ship CCGS “Louis S. St-Laurent”. The seismic source used along refraction/wide-angle reflection Line 3 (Fig. 1) was an airgun array consisting of six 1000 in.³ (16.4 L) guns towed at a depth of 6 m. This was the maximum number of airguns that could be safely towed in the ice infested waters. Instead of using a tuned airgun array with a smaller volume, it was decided to use guns with the maximum volume chambers to ensure that the signal was strong enough to be recorded at large offsets (>150 km). As a result, the data recorded are rather mono-frequent (maximum energy between 5-6 Hz) and have a tendency to ringing in the signal. The shot interval was 60 s at a ship’s speed of 4 knots, resulting in an average shot spacing of 128 m. Ice conditions prevented shooting in a 63 km long segment at the entrance to Makinson Inlet on Ellesmere Island (Fig. 1). The airgun array was triggered by a Global Positioning System (GPS) clock. Occasional periods with no satellite reception resulted in a few short shot gaps.

Eight digital ocean bottom seismometers (OBS) of the Geological Survey of Canada (GSC) were deployed along Line 3 with station numbers 8 through 15 (Fig. 1). Originally it was planned to have another OBS east of Cape Combermere (OBS 7), but it appeared too risky to deploy the instrument at that location due to large ice floes. All OBS were equipped with three-component 4.5-Hz geophones and a hydrophone (frequency range 0-5000 Hz) and the average spacing of the OBS was 20 km. Six ORION land stations with three-component 1-Hz geophones were deployed by the ship’s helicopters. Station 1 was located at Stenkul Fiord at western Ellesmere Island, stations 2 through 6 were placed along the southern shore of Makinson Inlet and at Smith Bay with an average spacing of 24 km, and station 16 was installed on Saunders Island off Greenland. In addition, we could utilize a broadband seismometer (GURALP CMG-40 seismometer with Nanometric ORION datalogger) located in Pituffik/Thule Air Base (station 17).

All navigation (station and shot locations) and timing (shots and recording) was based on the GPS system. Water depths along the profile were obtained from the ship’s echosounder using a depth-velocity function from one CTD (conductivity, temperature, depth) measurement in southern Nares Strait (78.33 °N, 73.64 °W) down to a depth of 662 m.

Data processing

All seismic data were converted to SEG-Y format, time corrections for the drift of the OBS clock were applied, and data were de-biased. Travel times of the direct wave were used to determine the exact position of the OBS at the seafloor, from which the shot-receiver ranges were calculated.

The maximum seismic energy was recorded between 5-6 Hz and the data were band-pass filtered from 4-10 Hz. To sharpen the wavelet and remove some of the ringing that resulted from the mono-frequent source, a deconvolution was applied. All record sections in Figures 2 through 11 are displayed with a

reduction velocity of 7.0 km s⁻¹ and traces are weighted by their distance to the station to increase the amplitudes for large offsets.

Methodology

For the two-dimensional velocity modeling along Line 3, all station locations were projected on a great circle arc running from station 1 at Stenkul Fiord to station 17 at Pituffik/Thule Air Base. In this framework, station 1 defines the origin of the horizontal axis ($x = 0$ km) and station 17 marks the eastern end at a range of $x = 377.57$ km. The velocity model for the crust and uppermost mantle was developed using the program RAYINVR (ZELT & SMITH 1992, ZELT & FORSYTH 1994). The uppermost layer in this model was the water column along the shot line. Static corrections were applied to the land stations to correct for their elevation. First, observed travel times of compressional phases (P waves) were fitted by forward modelling, with the model being developed from top to bottom. In a second step, velocities within individual layers were optimized using the inversion algorithm in RAYINVR. Layer boundaries were adjusted accordingly and the geometry of the Moho discontinuity was refined by inversion.

Finally, available shear-wave observations were used to develop a gross S wave velocity model of the crust. The S wave velocity model is defined by the P wave velocity model and assigned Poisson’s ratios for individual layers.

Seismic data

All instruments could be successfully recovered after the experiment. However, due to technical problems, station 4 did not work and station 1 did not record the shots fired in Makinson Inlet. In addition, station 5 was destroyed by a polar bear and only the shots in the eastern segment could be retrieved. This leaves the experiment with a reduced number of observations on Ellesmere Island (Fig. 1). During the shooting in Nares Strait, the wind speed was 50 km/h with gusts up to 100 km/h. This resulted in reduced signal-to-noise ratios and the OBS were most affected by these conditions. However, despite these impediments, a reasonable quality data set was collected.

Below a selection of record sections is discussed, which addresses some of the structures encountered along the line. The following phase nomenclature is used in the description. Refracted P waves within the five sedimentary layers are labeled P_{S1} through P_{S5} , reflections from the base of these layers are named $P_{S1}P$ through $P_{S5}P$. For refractions within the three crustal layers, the terms P_{c1} (upper crust), P_{c2} (middle crust), and P_{c3} (lower crust) are used; $P_{c1}P$ and $P_{c2}P$ are reflections from the base of the upper and middle crust, respectively. The crust-mantle boundary (Moho) is marked by P_mP reflections and refractions in the mantle are named P_n . Shear phases use the letter S instead of P .

Figure 2 illustrates some complexity encountered in the eastern part of Line 3. The refraction within sediment layer S3 (P_{S3}) has a phase velocity of 6.2 km s⁻¹. At an offset of 33 km, this phase fades out and the next visible refraction P_{c1} is delayed by c. 800 ms. This indicates a low-velocity zone (LVZ) underneath layer S3 down to the basement.

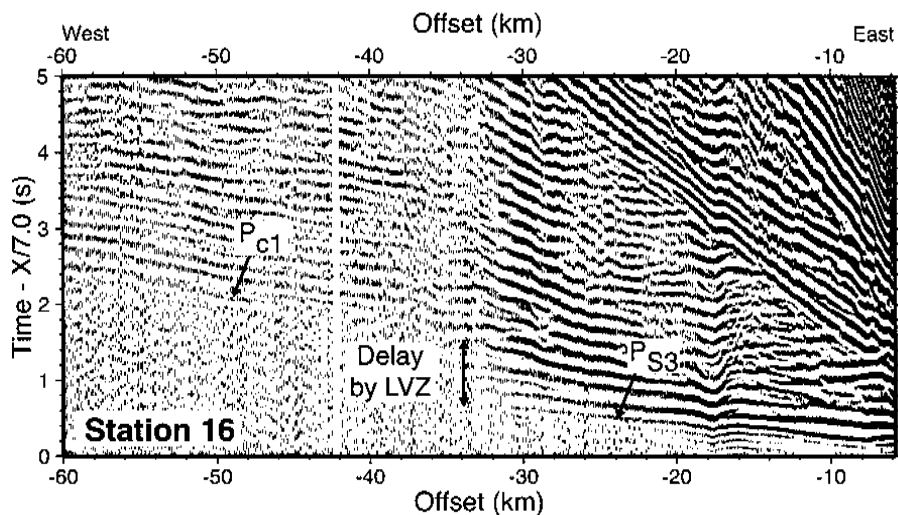


Fig. 2: Detail of record section for the vertical geophone component of station 16 (ORION land station, Saunders Island off Greenland). Horizontal scale is shot-receiver distance (offset) and the vertical scale is the travel time using a reduction velocity of 7.0 km s^{-1} . Processing includes a band-pass filter from 4 to 10 Hz. Traces are weighted by their distance to the station.

The following description of record sections begins in the east at Pituffik/Thule Air Base and moves subsequently westwards. Station 17 (Fig. 3) records the last part of a refraction within sediment layer S_2 (P_{S_2}) with a phase velocity of 4.8 km s^{-1} . The P_{S_3} refraction is very strong up to an offset of 33 km and continues weakly up to 45 km. A corresponding S phase (S_{S_3}) displays similar characteristics. The delay to the P_{c1} phase is caused by the LVZ as mentioned above. The Moho reflection P_mP can be identified between offsets of 40 and 210 km, defining large parts of the Moho geometry along the profile. Rather unusual is the observation of a P to S conversion at the Moho (P_mS) at 11.3 s reduced travel time with high amplitudes between 69 and 88 km on the vertical component. On the East-component, the phase is even more prominent. P_mS phases are thought to indicate a fairly sharp Moho transition relative to the incident P wavelength (GUEST et al. 1993). At offsets of c. 200 km, there are hints of a rather weak arrival ahead of the

P_mP with a phase velocity of 7.0 km/s . This observation matches the predicted arrival time of the P_{c3} .

Station 16 (Fig. 4) is located on Saunders Island close to the eastern end of Line 3. As discussed above the record is affected by the LVZ, causing the delay between the P_{S_3} and P_{c1} phases. The P_{S_3} has a high amplitude and so has the corresponding shear wave S_{S_3} . Although by definition no refractions from the LVZ can be observed, there is a strong reflection of the base of the LVZ ($P_{S_3}P$). The P_mP phase on station 16 is again characterized by high amplitudes, weak pre-critical P_mP arrivals can be identified as close as 24 km.

OBS 15 (Fig. 5) indicates a westward dip of sediment layer 3, as the P_{S_3} phase velocities are lower to the west ($<5.8 \text{ km s}^{-1}$) than to the east (6.5 km s^{-1}). P_{c1} arrivals show the characteristic jump relative to the P_{S_3} , indicating that the LVZ is still present.

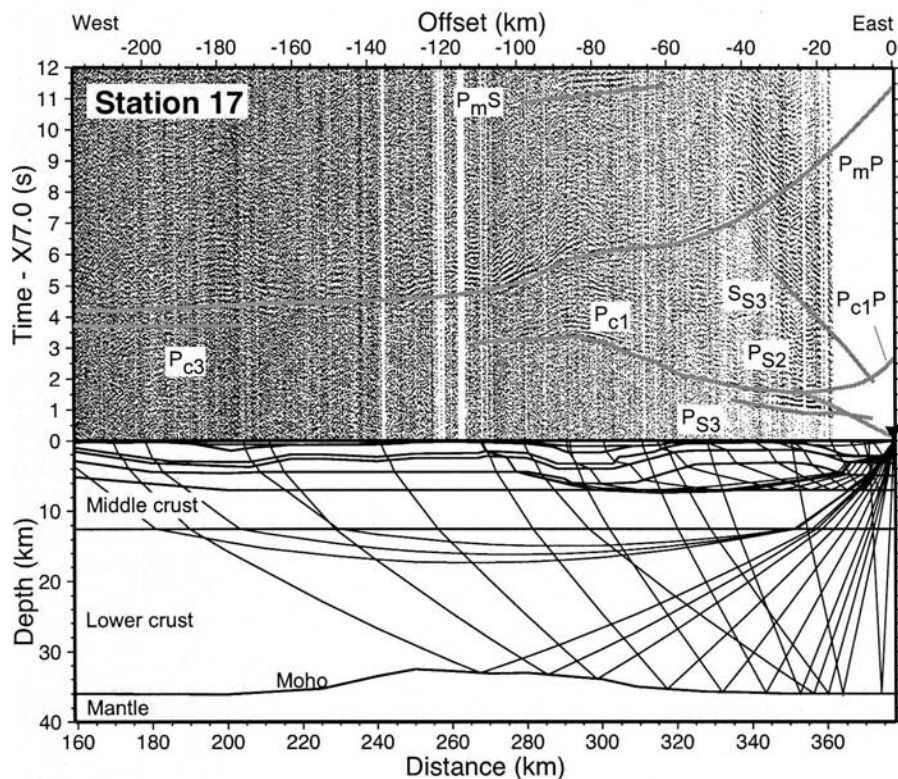


Fig. 3: Record section with computed travel times (top) and ray path diagram (bottom) for the vertical geophone component of station 17 (broadband seismometer in Pituffik / Thule Air Base). Horizontal scale in the record section is shot-receiver distance (offset) and the vertical scale is the travel time using a reduction velocity of 7.0 km s^{-1} . A triangle indicates the receiver location. See text for description of phases. The horizontal scale in the ray path diagram is distance along the velocity model.

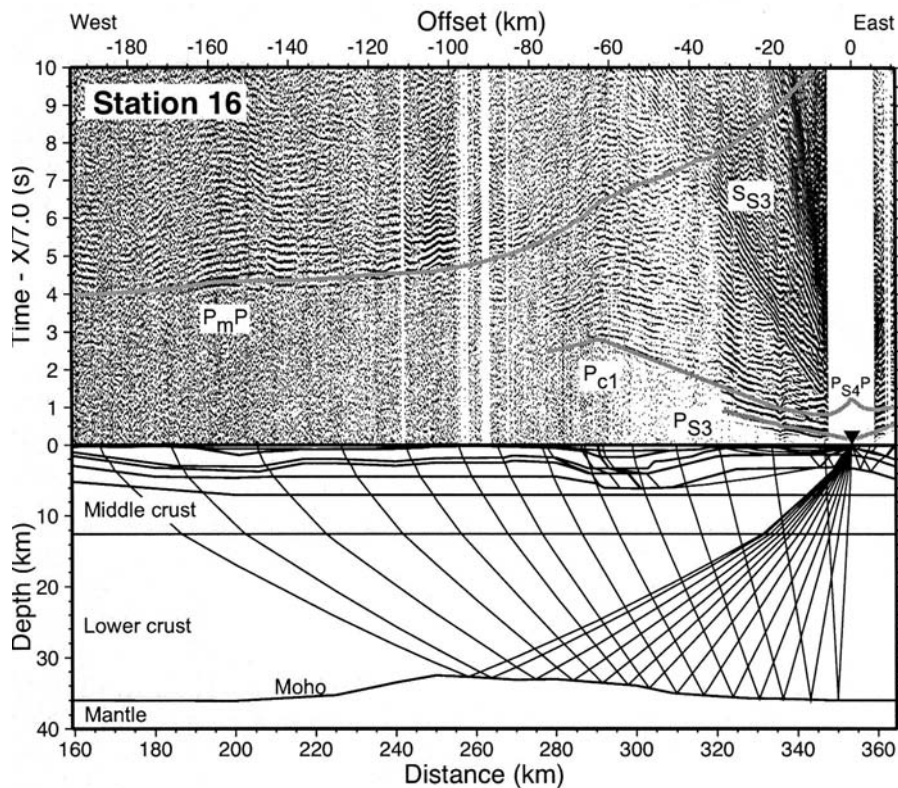


Fig. 4: Record section with computed travel times (top) and ray path diagram (bottom) for the vertical geophone component of station 16 (ORION land station, Saunders Island off Greenland). For further details see Figure 3.

The P_mP phase is still recognizable as a high amplitude phase but the signal-to-noise ratio is less than at the neighbouring land station 16, indicating that the impact of the stormy weather was more severe on the OBS records.

At OBS 13 (Fig.6), high noise levels and complexities associated with the LVZ prevent a reliable phase correlation at

offsets >60 km. Nevertheless, three refractions (P_{s1} through P_{s3}) can be identified, as well as some energy from crustal reflections ($P_{c1}P$ and $P_{c2}P$). The refraction within the uppermost layer (P_{s1}) has a phase velocity of 3.1 km s^{-1} . This layer occurs at two isolated basins only, and OBS 13 has the best record of it because the layer has its maximum thickness there.

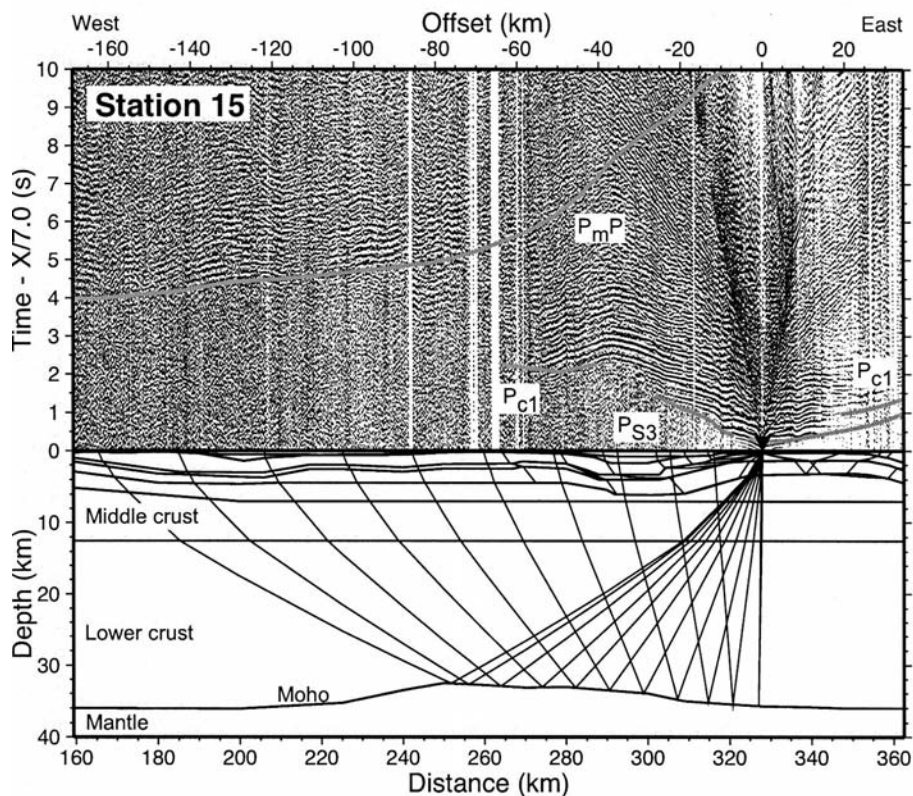


Fig. 5: Record section with computed travel times (top) and ray path diagram (bottom) for the hydrophone component of station 15 (easternmost OBS). For further details see Figure 3.

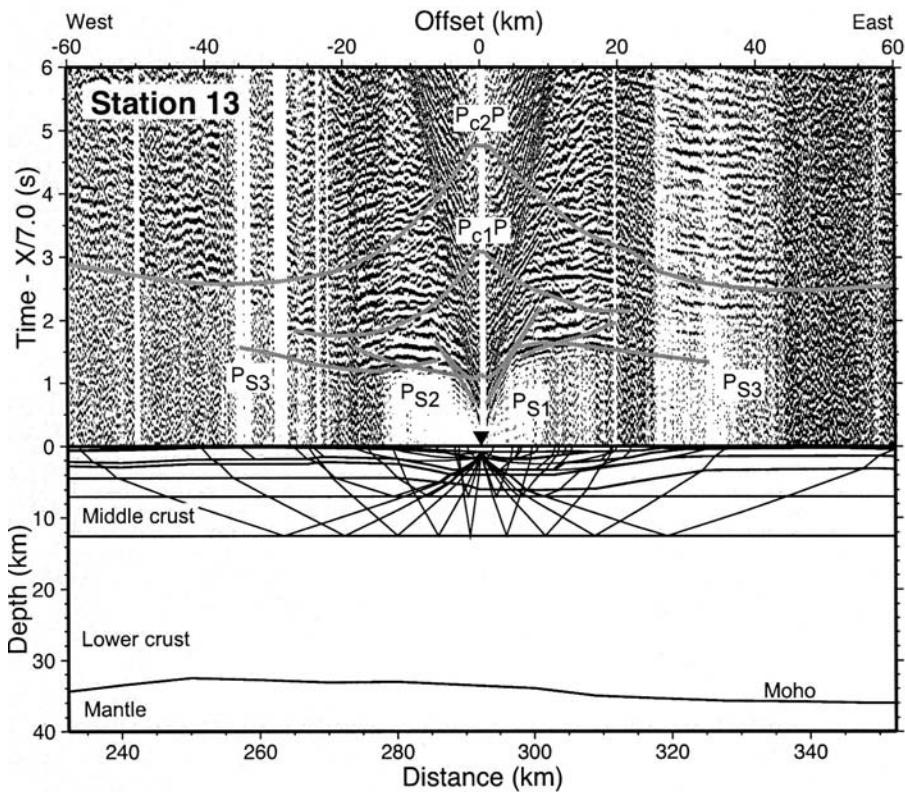


Fig. 6: Record section with computed travel times (top) and ray path diagram (bottom) for station 13 (OBS in eastern Nares Strait). For further details see Figure 3.

For OBS 9 (Fig. 7) the signal-to-noise ratio is improved again. Along the shot segment in Makinson Inlet, the Moho reflection P_mP can be identified. OBS 8 (Fig. 8) shows clear P_mP reflections to either side of the instrument. However, no clear P_{cl} phase is recognizable on that record section. To the west, this could be related to the shot gap off Ellesmere Island at offsets where the P_{cl} phase would be expected. Its absence to

the east may be related to complications associated with the LVZ. The velocity within the upper crustal layer might be slightly lower than in the high velocity sediment layer 3, preventing upper crustal refractions. Comparison between phase velocities of the P_{cl} and P_{S3} at other stations shows similar values around 6.0 km s^{-1} , in support of this explanation.

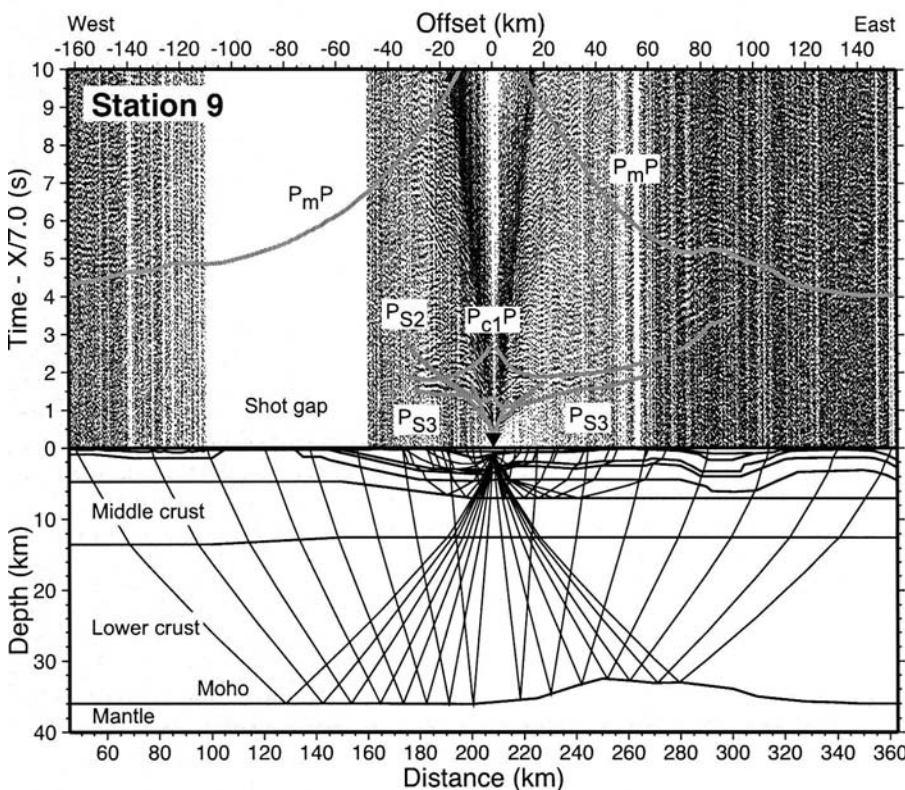


Fig. 7: Record section with computed travel times (top) and ray path diagram (bottom) for the vertical geophone component of station 9 (OBS in western Nares Strait). For further details see Figure 3.

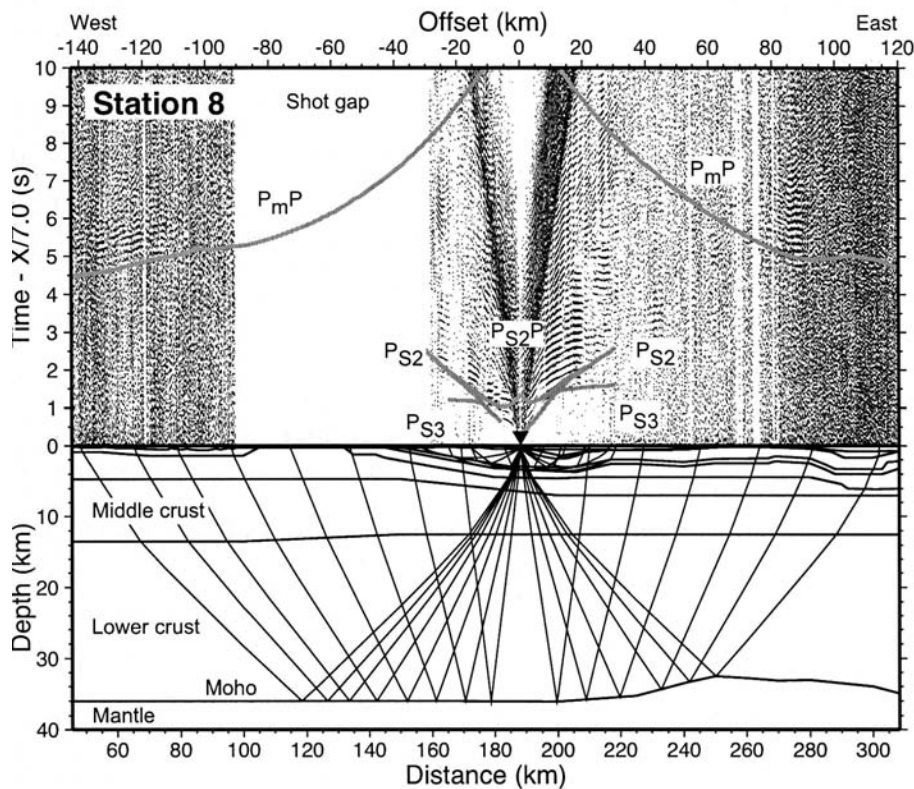


Fig. 8: Record section with computed travel times (top) and ray path diagram (bottom) for the hydrophone component of station 8 (westernmost OBS). For further details see Figure 3.

Stations on Ellesmere Island are not affected by the complications associated with the LVZ in the Thule Basin. Land station 3 (Fig. 9) recorded both refractions from within the upper and middle crust (P_{c1} and P_{c2}) up to offsets of 160 km. The record also exhibits a strong P_mP phase and has the clearest P_n phase of all stations. The mantle refraction can be correlated from 130 to 300 km with the highest amplitudes observed at offsets

of 200 to 230 km. The station is not located on basement (upper crust) as can be seen by an additional refraction P_{S5} that comes in before the P_{c1} phase. The phase velocity of the P_{S5} is around 5.0 km s^{-1} .

Station 2 (Fig. 10) at the westernmost end of Makinson Inlet has an excellent signal-to-noise ratio and recorded both high-

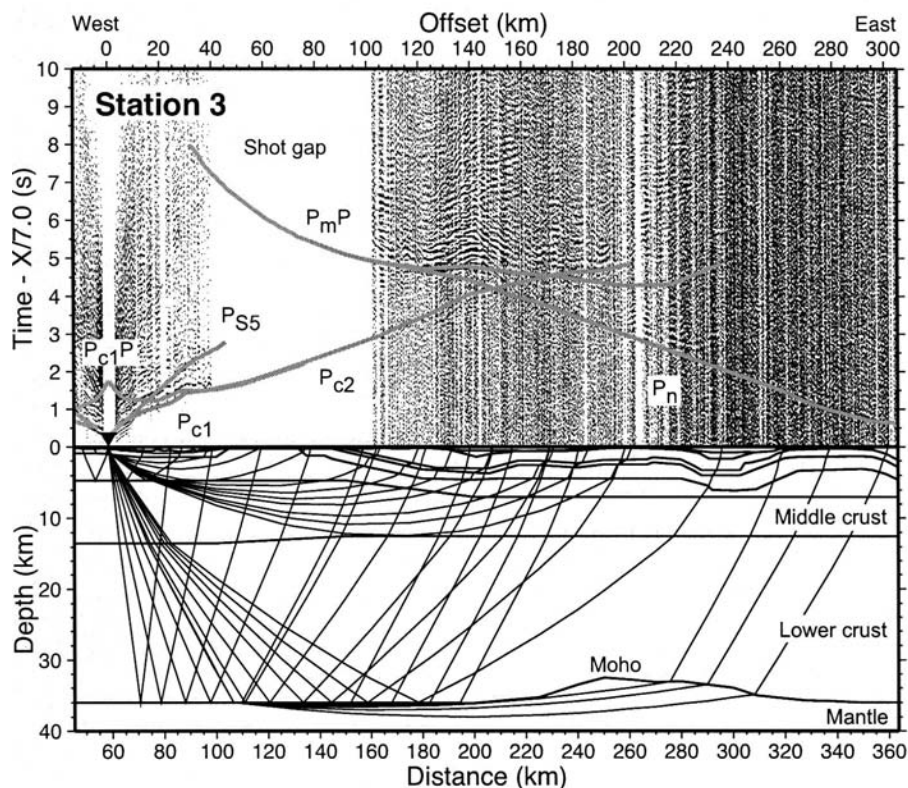


Fig. 9: Record section with computed travel times (top) and ray path diagram (bottom) for the vertical geophone component of station 3 (ORION land station, western part of Makinson Inlet). For further details see Figure 3.

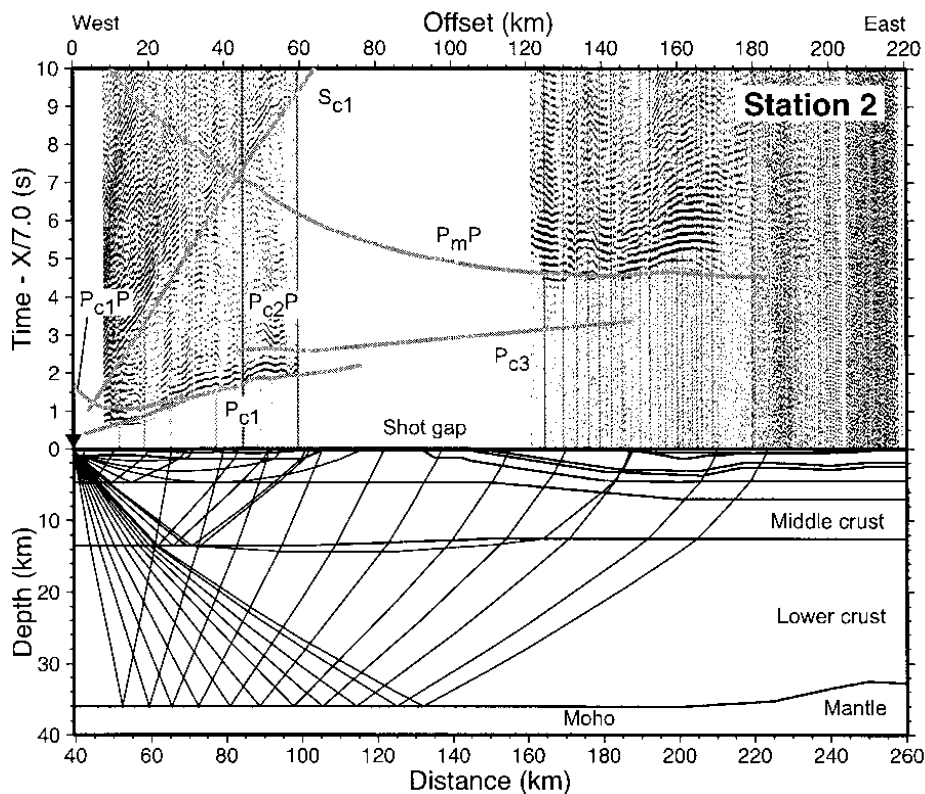


Fig. 10: Record section with computed travel times (top) and ray path diagram (bottom) for the vertical geophone component of station 2 (ORION land station, westernmost station at Makinson Inlet). For further details see Figure 3.

amplitude P and S refractions from within the upper crust (P_{cl} and S_{cl}). Just before the major shot gap, a strong phase follows the P_{cl} at an offset of 52 km. It could be either a reflection ($P_{c2}P$) or more likely a diffraction from the mid-crustal boundary based on calculations from the velocity model. To the east of the shot gap, a weak refraction can be correlated, which is interpreted as P_{c3} phase, followed by strong P_mP reflections.

Modelling of station 1 (Fig. 11) was difficult, because of the instrument's failure to record the shots in Makinson Inlet; the closest shot was at an offset of 161 km. When the velocity model is continued horizontally from station 2 towards station 1, the calculated arrival times of the P_mP phase appear to come in ca. 700 ms too early, if the moderate amplitude phase between 160 and 180 km is indeed the P_mP . A better fit can be achieved in many ways, e.g. by a deepening of the Moho, a

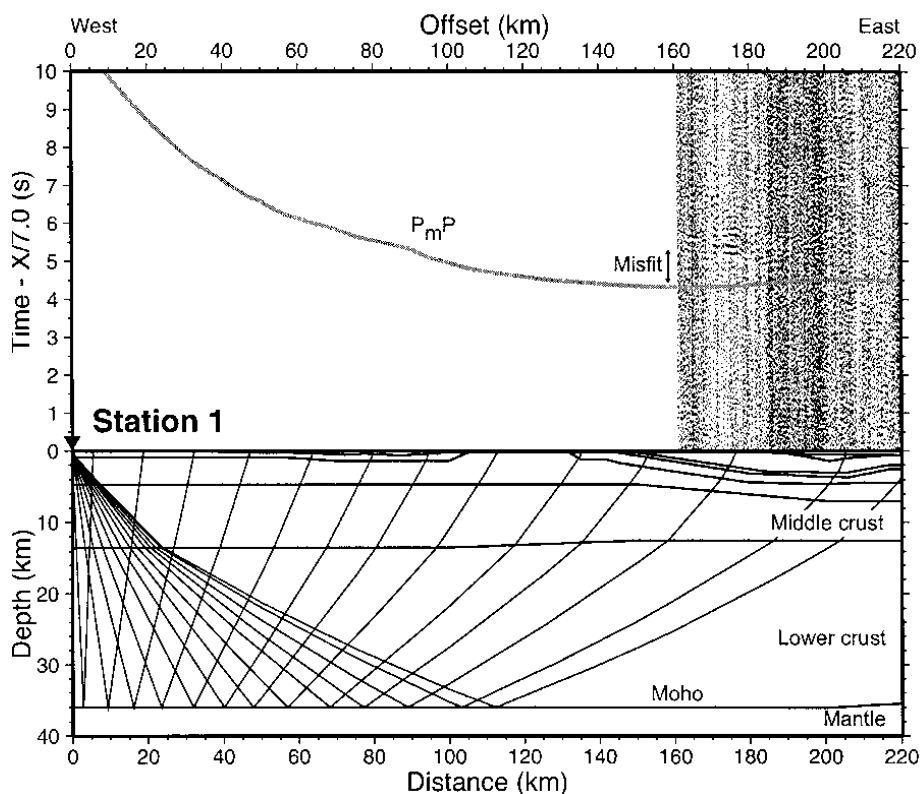


Fig. 11: Record section with computed travel times (top) and ray path diagram (bottom) for the vertical geophone component of station 1 (ORION land station at Stenkul Fiord, eastern Ellesmere Island). For further details see Figure 3.

reduction of crustal velocities west of station 2 or by introducing thicker/slower sediment layers around station 1. None of these alternatives can be confirmed by the seismic data due to the lack of observations, in particular lack of reverse observations, and therefore no attempt was made to improve the travel time fit for this instrument. The remaining stations not discussed in this section are shown with the ray-tracing and travel time curves in Figure 12.

RESULTS

Velocity model

The velocity model (Fig. 13) shows a 5-km thick sediment package consisting of three individual layers (sediment layers 2 through 4) between km 132 and 378. This package is interpreted to represent the Thule Supergroup (Thule Basin). The uppermost layer (sediment layer 2) is ~2 km thick, P wave velocities range from 4.5 to 5.0 km s^{-1} , and the Poisson's ratio is 0.30. The velocity of the middle layer (sediment layer 3) is 6.1 km s^{-1} and its Poisson's ratio is 0.28. The thickness of this layer is not very well determined, since no reflections from its base were observed and the velocity inversion prevented refractions in the underlying layer. However, to model the range of the P_{S3} phase, lateral thickness variations were required. The model uses a thickness of 1000 m in the east and 400 m in the west giving a general sense of the lateral

thickness variations in this layer. Due to the low velocity zone, no velocity information was obtained from within the lowermost layer in the Thule Group (sediment layer 4). In the model, we are assuming a velocity of 5.05 km s^{-1} , which presents the downward continuation of velocities found in the upper layer (4.5-5.0 km s^{-1}). The base of the Thule Group is defined by occasional reflections ($P_{S4}P$) and by crustal refractions (P_{c1}), locating it at a depth between 4.4 and 6.2 km, before the Thule Basin thins westwards and eventually disappears at km 132. However, these depth values depend on the velocities in sediment layer 4.

Within the Thule Supergroup, two isolated sedimentary basins (sediment layer 1) can be identified with lower velocities. One of these basins is located at km 200 with velocities of 3.2 km s^{-1} . Its maximum thickness is 800 m. The other basin extends from km 280 to 310 with a maximum thickness of 900 m and velocities of 2.9 km s^{-1} . West of km 105, a 900 m thick layer (sediment layer 5) with a velocity of 5.05 km s^{-1} was introduced to explain the delay of crustal refractions in the area of Makinson Inlet.

The crust is divided into three layers. The base of the upper crust is at a depth of 4.7 km west of km 150 and at a depth of 7.0 km in the eastern part. Velocities range from 5.95-6.05 km s^{-1} in the west to around 6.15 km s^{-1} in the east. The Poisson's ratio in the upper crust is 0.25. Velocities in the middle crust are around 6.1 km s^{-1} in the west and 6.2 km s^{-1} in the east with

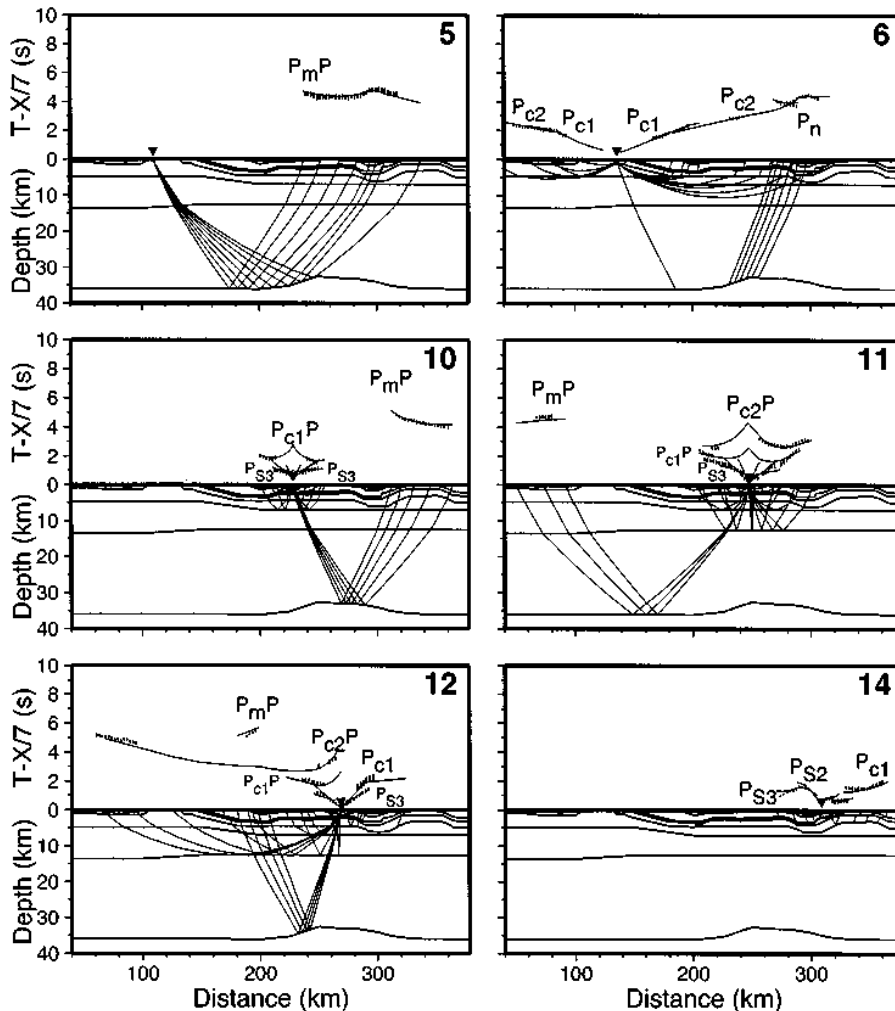


Fig. 12: Comparison of observed and calculated travel times for stations 5, 6, 10, 11, 12, and 14, shown together with the corresponding ray paths. Observed data are indicated by vertical bars with heights representing pick uncertainty; calculated data are indicated by solid lines. Triangles mark the receiver locations. Horizontal scale is the model position; a reduction velocity of 7.0 km s^{-1} has been applied for the travel times.

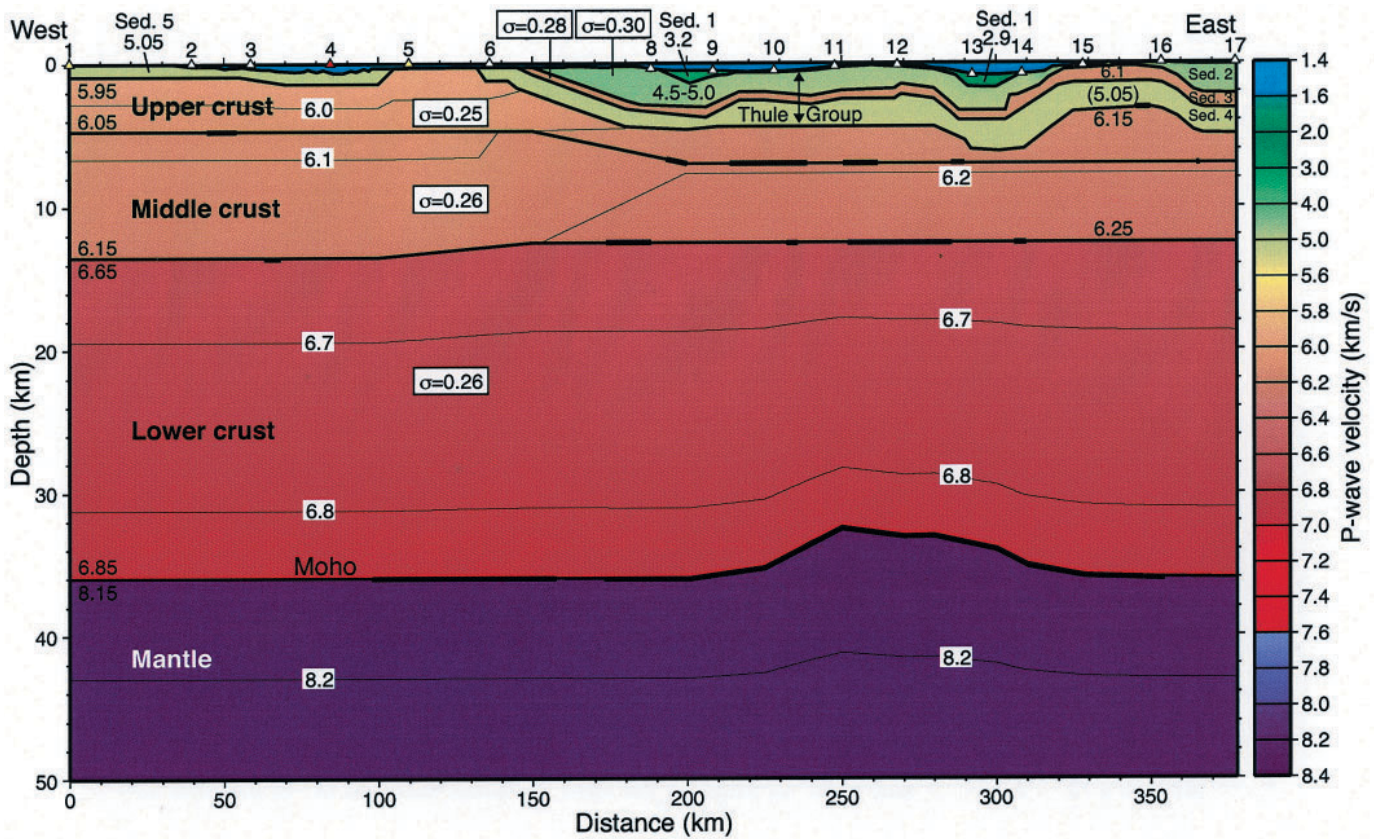


Fig. 13: *P* wave velocity model with a contour interval (thin solid lines) of 0.1 km s⁻¹ between 5.9 and 8.3 km s⁻¹. Numbers indicate velocity in km/s. Layer boundaries constrained by reflections are drawn with bold solid lines. Triangles mark the location of receivers (white indicates that all shots were recorded; yellow indicates that the shots in Makinson Inlet were not recorded; red means no data recovery). For some layers, the Poisson's ratio (σ) is specified. Sed. = sedimentary rocks.

a Poisson's ratio of 0.26. The mid-crustal boundary, which separates middle and lower crust is located at a depth of 13.5 km in the west and 12.5 km in the east. Lower crustal velocities do not show lateral variations, they are 6.65 km s⁻¹ at the top and 6.85 km s⁻¹ at the bottom of the layer with a Poisson's ratio of 0.26.

The crust-mantle boundary is at a depth of 36 km but shallows slightly between km 210 and 330 where a minimum Moho depth of 33 km is found. Velocities in the uppermost mantle are best modelled with 8.15 km s⁻¹.

Model Resolution and uncertainty

Travel time residuals, number of observations, and normalized χ^2 for individual phases are summarized in Table 1. The total root-mean-square (rms) misfit is 151 ms. The estimated pick uncertainty varied between 50 ms for high-amplitude observations close to the stations to 250 ms for low-amplitude arrivals at larger offsets. The χ^2 of the experiment is 2.247, compared to the optimum value of 1.0, when all arrivals are modelled within the given pick uncertainties. The rather high χ^2 value in this study is mainly attributed to the complex velocity structure in the upper few kilometres of the model, which made the ray tracing difficult. Often head waves had to be used instead of refracted waves to obtain the desired ray coverage. These difficulties are related to the low velocity zone (LVZ) encountered in sediment layer 4. The fact that the velocities above and below the LVZ are very similar, added to the ray tracing problems. In addition, sediment layer 3 was very sensitive to

changes in the model because refractions (P_{s3}) within this rather thin layer often were required to propagate for 40 or more kilometres.

Figure 14 shows the values of the diagonal of the resolution matrix for the velocity nodes of the model. Ideally, these values are 1, with values <1 indicating spatial averaging of the true Earth's structure by a linear combination of model parameters (ZELT 1999). Resolution matrix diagonals of greater than 0.5-0.7 indicate reasonably well resolved model parameters (LUTTER & NOWACK 1990). Using this definition, the westernmost part of the model is poorly constrained. This is

Phase	n	t_{rms} (ms)	χ^2
P_{s1}	53	0.061	0.668
$P_{s1}P$	7	0.027	0.085
P_{s2}	163	0.079	1.007
$P_{s2}P$	21	0.104	1.161
P_{s3}	556	0.118	2.011
$P_{s3}P$	31	0.128	4.282
P_{s5}	6	0.051	1.247
P_{v1}	445	0.116	1.740
$P_{c1}P$	187	0.104	1.141
P_{c2}	219	0.173	2.324
$P_{c2}P$	262	0.155	1.845
P_{c3}	24	0.115	0.677
P_mP	1243	0.185	3.269
P_n	210	0.140	0.853
All phases	3427	0.151	2.247

Tab. 1: Number of observations (n), RMS misfit between calculated and picked travel times (t_{rms}), and normalized χ^2 for individual phases.

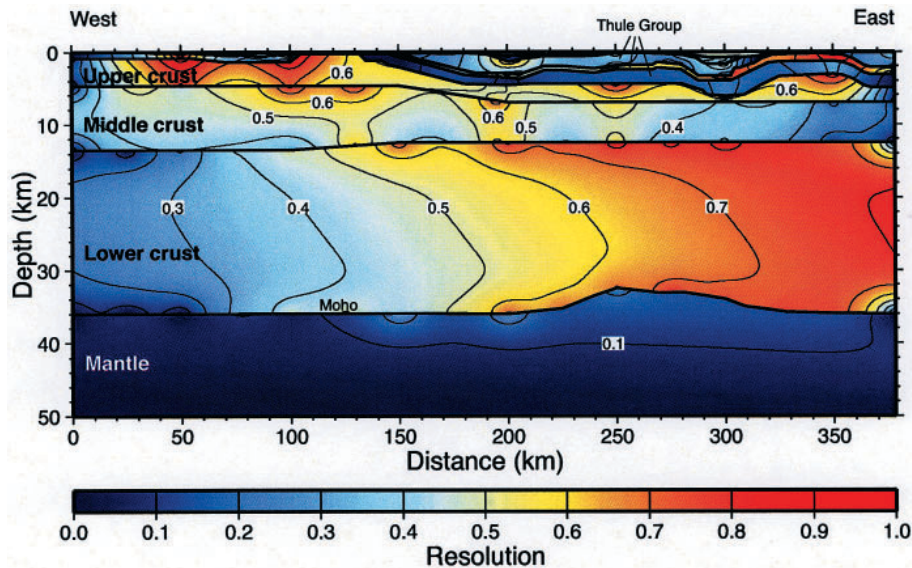


Fig. 14: Diagonal values of the resolution matrix of the P wave velocity model displayed in contour format (0.1 contour interval).

related to shot gaps and station failures in that area. Sediment layers 1 and 2 are also poorly resolved due to the lack of reversed ray-path coverage. However, since the geometry of these two layers is mostly defined by the seafloor, the uncertainty is less than what the formal resolution analysis indicates. Sediment layer 3 (high-velocity basalt layer) is well constrained, while velocities in the underlying low-velocity zone (sediment layer 4) are not resolved.

Upper crustal velocities are well resolved, while reasonable resolution in the mid-crustal layer is restricted to the area between 60 and 210 km. This reflects the lack of P_{c2} arrivals in most parts of the model. Also P_{c3} phases are scarce. However, here the numerous Moho reflections observed over long distances result in a well-resolved lower-crustal velocity structure east of c. 150 km. Resolution in the mantle is again reduced because long branches of the P_n phase were only observed on OBS 3 (Fig. 9). However, since the Moho geometry is well constrained, the mantle velocity cannot be varied too much.

Another way to estimate the uncertainties of the model is to vary individual velocity and boundary nodes and check how much they can be varied without a significant increase in the travel time residuals. The LVZ itself is unconstrained in velocity, except that it must be lower than in the overlying sediment layer 3. Since sediment layer 3 appears to be intercalated to the Thule Group, it seems fair to assume that the velocity in sediment layer 4 is similar to layer 2. This leaves a total spectrum of 5.0–6.1 km s⁻¹ as possible velocities for layer 4. The depth of the base of the Thule Group depends on this velocity. If the layer 4 velocity were 6.1 km s⁻¹, the Thule basin would be ~450 m deeper. Variations within other layers yield estimates that the velocities within sediment layers 1, 2, 3, and 5 are accurate within ± 0.1 km s⁻¹. In the upper and middle crust, the allowable change in velocity is ± 0.15 km s⁻¹, and in the lower crust and mantle ± 0.1 km s⁻¹.

Segments of layer boundaries that are mapped by reflections are shown as bold lines in Figure 13. This shows that almost the entire Moho east of km 100 is well constrained and cannot be changed by more than ± 1 km without increasing the travel time residuals. The layer boundaries between upper/middle

crust and between middle/lower crust are less well mapped and can be varied by up to 2 km. The S wave arrivals are sensitive to changes in Poisson's ratio > 0.01 .

Gravity Modelling

Two-dimensional gravity modelling (TALWANI et al. 1959) was performed along the line to verify how consistent the velocity model is with the gravity data. Gravity anomalies were extracted from the map of O'KEY et al. (2001). The density model was derived from conversion of P wave velocities to density using the empirical relation of Ludwig, NAFE & DRAKE (1970) that is approximated by

$$\rho = -0.00283 \cdot v^4 + 0.0704 \cdot v^3 - 0.598 \cdot v^2 + 2.23 \cdot v - 0.7$$

with ρ the density in g cm⁻³ and v the P wave velocity in km s⁻¹.

Results of the gravity modelling are shown in Figure 15 and indicate a reasonable match between the calculated and observed gravity. There is some misfit but the positions and shape of the gravity highs and lows are matched. No attempt was made to modify the model in order to improve the fit. The reason for this is that the structure is not two-dimensional as can be seen on the gravity map in Figure 16. For example, close to OBS 8 and 9, there is a lateral change of the gravity signature. To the north of line 3 there is a gravity low (-80 mgal), while immediately to the south a gravity high with values of up to 80 mgal is encountered. Similar north-south variations occur at the Carey Islands and between OBS 13 and 14. Other problems can be expected at either end of line 3. At the eastern end of line 3, the Thule Supergroup is 5 km thick and this is the value the gravity model was extended with to infinity to avoid edge effects. However, as the geology map (Fig. 1) indicates, the Thule Group disappears ca. 30 km to the east of line 3. At the western end of line 3, the continuation of the density model to infinity has some problems, too. As discussed above, the velocity model is not constrained very well for station 1 and the $P_m P$ phase indicates some misfit (Fig. 11 and discussion in 3.4). So it is no surprise that the gravity model has the largest misfit at the western end.

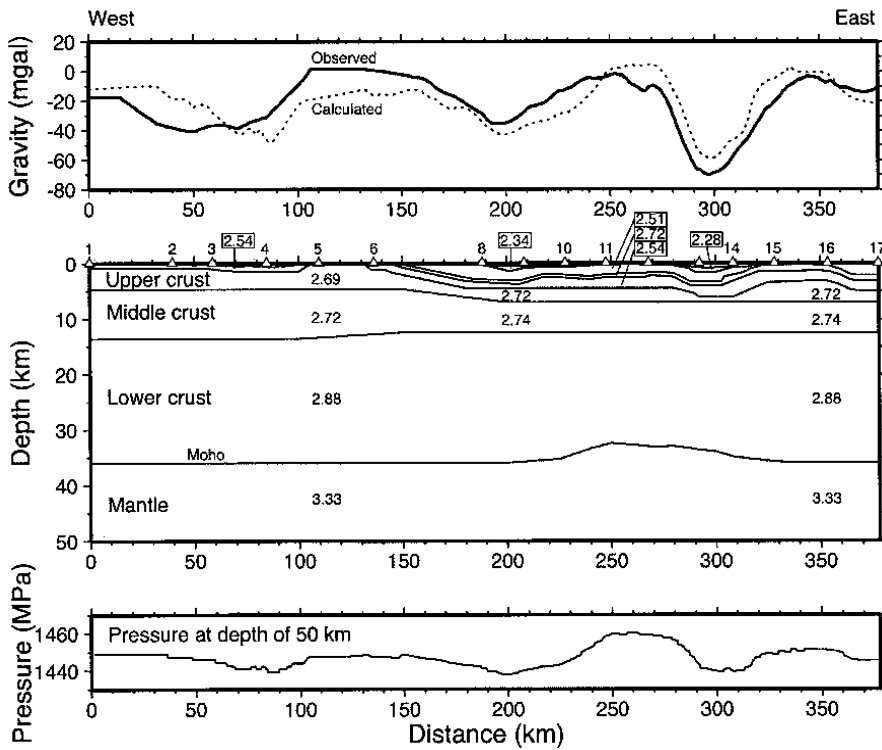


Fig. 15: Two-dimensional gravity modelling for Line 3. The P wave velocity model (Fig. 13) was converted to density using the velocity-density relationship of LUDWIG et al. (1970). Densities in the model (middle) are given in g cm^{-3} , triangles mark the OBS positions. Observed and calculated gravity anomalies (top) are shown by solid and dashed lines, respectively. The lithostatic pressure (bottom) at the base of the model (depth of 50 km) is shown as solid line.

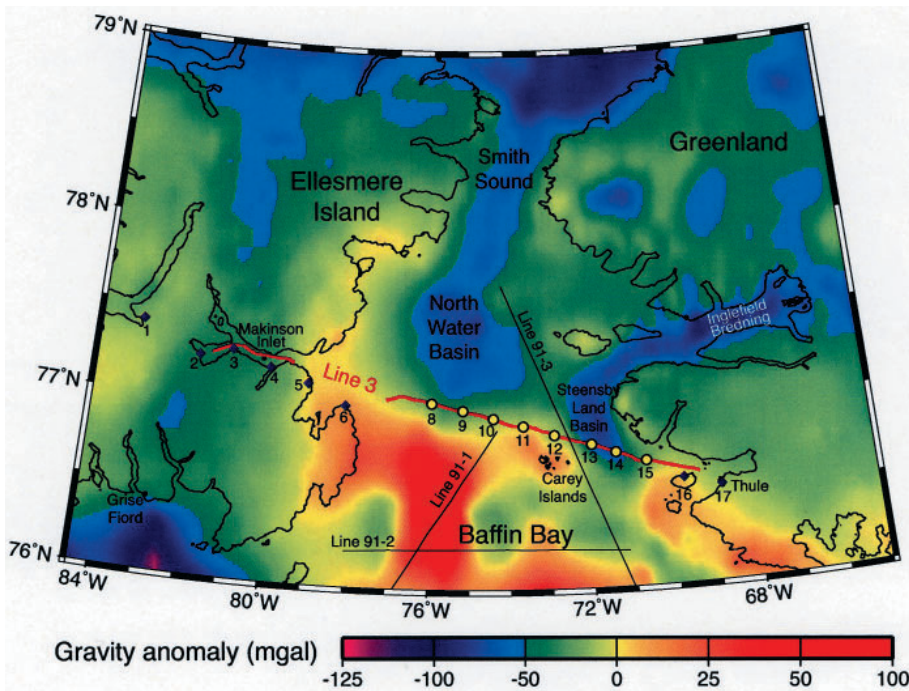


Fig. 16: Gravity anomaly map (data from OAKEY et al. (2001)). Offshore areas are presented by free-air gravity, land areas represent Bouguer gravity anomalies. Red line = shot segments of Line 3; yellow circles = position of OBS; blue diamonds = location of seismic land stations. Refraction seismic lines relevant to this study are shown by solid lines; lines 91-1 and 91-3 (JACKSON & REID 1994), lines 91-2 and 91-4 (REID & JACKSON 1997).

Figure 15 also shows the lithostatic pressure at the base of the model (50 km). The average pressure is 1450 MPa with variations of ± 10 MPa, indicating that the model is approximately isostatically balanced at its base. The most pronounced deviation occurs in the area with the reduced crustal thickness in the vicinity of the Carey Islands (km 240 to 280).

DISCUSSION

Thule Group

The velocity model (Fig. 13) shows that the Thule Supergroup

is a continuous feature that can be correlated from Greenland across Nares Strait to Ellesmere Island, where it thins and disappears at Cape Combermere (Fig. 1). The most intriguing feature within the Thule Basin is certainly the interbedded high-velocity layer with velocities around 6.1 km s^{-1} . A Poisson's ratio of 0.28 indicates a rather mafic composition of this layer and CHRISTENSEN & MOONEY (1995) specify the average P wave velocity of basalts at a depth of 5 km as 5.85 km s^{-1} (standard deviation of 0.55 km s^{-1}). A basaltic composition of the 6.1-km s^{-1} layer in the Thule Group therefore appears likely. We assume that the layer correlates with the Cape Combermere Formation (DAWES 1997); a formation that consists of a complex suite of effusive, hypabyssal and

pyroclastic basaltic rocks with interbedded water-lain volcanoclastic and clastic sediments and subordinate siliciclastic carbonate rocks. Individual sills are up to 140 m thick. The formation is exposed at Cape Combermere on Ellesmere Island, in the vicinity where the high-velocity layer outcrops / disappears on line 3 (Fig. 13).

Velocities within the upper layer of the Thule Basin (sediment layer 2, Fig. 13) of 4.5 to 5.0 km s⁻¹ and a Poisson's ratio of 0.30 are compatible with a high content in carbonates. This is consistent with rocks found on Saunders Island, the location of land station 16. Here the Narssârssuk Group is characterized by a cyclic arrangement of siliciclastic and carbonate units (DAWES 1997). Velocities within the lower layer of the Thule Basin (sediment layer 4, Fig. 13) are not constrained because they represent a low velocity zone. However, with the overlying layer interpreted as Cape Combermere Formation, sediment layer 4 should represent rocks of the lower Nares Strait Group, the Northumberland Formation. The dominant lithologies are sandstones, mainly quartz arenites, with shale and siltstone units (DAWES 1997).

The P_{s3} refractions from the unit interpreted as Cape Combermere Formation are the phases that are best recognized on the record sections and they make sediment layer 3 to be a marker horizon in the velocity model (Fig. 13). The top of the layer is well defined east of OBS 8 and shows some depth variations indicating flexure within the Thule Basin. East of OBS 12, the character of the flexure indicates horst and graben structures. The region between km 285 and 315 is interpreted as a graben while the neighboring area from km 315 to 360 appears as a horst with uplift. In this zone, the high-velocity layer of the Cape Combermere Formation is almost exposed at the surface. Horst and graben structures are also known from the onshore geology of the Thule Group in Greenland (DAWES 1997).

Two sedimentary basins (sediment layer 1) overlie the Thule Basin. The basin around km 200 is at the southern tip of the gravity low that correlates with the North Water Basin (Fig. 16) mapped by JACKSON et al. (1992). The age of the deposits in the basin is unknown. The other basin around km 295 has P wave velocities of 2.9 km s⁻¹ and correlates well with another gravity low that continues into Inglefield Bredning (Fig. 16). The southwestern part of this basin was first defined by NEWMAN (1982) and subsequently called Steensby Land Basin. Again, the age of the strata in the basin is unknown. KEEN & BARRETT (1973) suggest that the basin and the associated physiographic low are due to erosion by glaciation with partial infilling by recent sedimentation. Presently, active glaciers are located at the eastern tip of Inglefield Bredning. In contrast, HARRISON (2006) correlates the Steensby Land Basin into the North Water Basin (Fig. 1).

Crustal variations across Nares Strait

Rocks within the upper and middle crust of Line 3 are characterized by P wave velocities of 6.0-6.3 km s⁻¹ and by a Poisson's ratio of 0.25-0.26 (Fig. 13). These properties fit well with those of granite (6.1 km s⁻¹ ± 0.2, Poisson's ratio $\sigma = 0.24 \pm 0.04$), felsic gneiss (6.2 km s⁻¹ ± 0.2, $\sigma = 0.25 \pm 0.03$), quartz-mica schists (6.3 km s⁻¹ ± 0.1, $\sigma = 0.26 \pm 0.04$) or granodiorite (6.1 km s⁻¹ ± 0.4, $\sigma = 0.27 \pm 0.02$) using the compilation of HOLBROOK et al. (1992). These rock types are compatible with

those typically encountered at the basement of NW Greenland, that are gneiss, schists and granites (DAWES 1976).

North of Line 3, Precambrian granitic gneiss was recovered on the Greenland side of North Water Basin and measurements of this sample gave a P wave velocity of 6.2 km s⁻¹ (NEWMAN 1982). This agrees with our upper crustal velocities of 6.2 km s⁻¹ in that area, and our Poisson's ratio is also consistent with a gneissic composition.

Lower crustal rocks along Line 3 have velocities between 6.65 and 6.85 km s⁻¹ and a Poisson's ratio of 0.26. These values plot between intermediate granulite (6.4 km s⁻¹ ± 0.2, $\sigma = 0.27 \pm 0.03$) and metapelite/granulite (7.2 km s⁻¹ ± 0.4, $\sigma = 0.27 \pm 0.01$) (HOLBROOK et al. 1992). Hence, we estimate that the lower crust is composed of granulites.

The velocity model of line 3 (Fig. 13) shows a uniform velocity structure consistent with the crustal composition found within the shield of northwest Greenland. This lateral homogeneity strongly suggests that the shield on either side of Nares Strait belongs to the same geological province. Any lateral change in the velocity structure could have argued in favour of a plate boundary or of strike-slip movement in Nares Strait in response to the northward movement of Greenland relative to North America, as predicted by plate reconstructions (ROEST & SRIVASTAVA 1989).

REID & JACKSON (1997) suggested a transform plate boundary in southern Nares Strait based on their refraction seismic line 91-2 some 80 km to the south of Line 3 (Fig. 1). They locate the plate boundary within the Carey Basin, where they see a minimum crustal thickness of 7 km compared to up to 20 km along the remainder of the line. The thickness of the sediments in the Carey Basin is 10 km and additional evidence for strike-slip movement was taken from seismic reflection records showing flower-structures as indication for transpression (JACKSON et al. 1992). The suggested transform plate boundary extends from Carey Basin to the North Water Basin (REID & JACKSON 1997) and would therefore coincide with the 1 km deep sedimentary basin at km 200 on Line 3 (Fig. 13). At this position there is no evidence for a shallowing of the Moho as seen on line 91-2. The Moho stays flat at a depth of 36 km. Also there is no jump in the geometry of the Thule Group or of other layer boundaries that could indicate strike-slip motion.

Based on the velocity model of Line 3, the most likely position of a transform plate boundary would be in the area of the Moho uplift between km 250 and 300, where the young sedimentary basin (sediment layer 1) and graben structure within the Thule Group is observed at km 300. However, the trend of this basin does not follow Nares Strait but turns towards Greenland as seen by the associated gravity low (Fig. 16). The shallowing of the Moho is interpreted to be a local feature and not a linear trend that could delineate a transform plate boundary. The gravity map (Fig. 16) reveals a circular pattern around the Carey Islands that correlates with the change in Moho depth as seen in the gravity modelling (Fig. 15). The shallowing of the Moho is interpreted to be associated with uplift at the Carey Islands and the age of this uplift is probably older than 120 Ma based on apatite (U-Th) He data (pers. comm. A. Grist 2003). This predates the opening of the Labrador Sea, with sea-floor spreading starting around 92 Ma (ROEST & SRIVASTAVA 1989). Hence, given the circular shape

and the age, it appears unlikely that the observed Moho shallowing on Line 3 is associated with a transform boundary between Greenland and North America.

Studies of other transform faults may provide an idea how the movement along the fault may affect the crustal structure. A refraction seismic study across the Dead Sea Transform (DESERT Group et al. 2004) shows an offset of the seismic basement by 3-5 km under the fault. Moho depth is affected within a 40-km-wide zone with a maximum shallowing of 2 km. Crustal velocities do not change across the fault. These results indicate that a transform fault is most likely detected by variations of the layer geometry. Variations of such dimensions are observed in our velocity model (Fig. 13) but a relation to a transform fault is dismissed (see above). If there was a transform fault in Nares Strait with similar characteristics as the Dead Sea Transform, seismic resolution should have been sufficient to recognize the fault.

Given the continuity in the nature of the crust and the undisturbed correlation of a 5 km thick sequence of sediments of the Thule Supergroup across Nares Strait, we suggest that the shield of southwestern Ellesmere Island could be part of the Greenland plate. In this case, the plate boundary should be located west of the Archean/Proterozoic shield, which is approximately west of station 3 (Fig. 1). This is also the region that is least constrained in our velocity model. The record section of station 1 (Fig. 11 and discussion in below) indicates some changes in the velocity model at the western end of the line, which is not surprising given the changing surface geology. However, the resolution of the data in the westernmost portion of Line 3 is not sufficient to map lateral velocity variations.

Comparison with other studies

Other available refraction seismic data in the vicinity of Line 3 include the four lines from the 1991 experiment. Lines 91-1

and 91-3 (JACKSON & REID 1994) are the most relevant lines since they cross or lie within the immediate vicinity of Line 3. Figure 17 summarizes some velocity-depth profiles of these lines for comparison with Line 3. At the crosspoint of lines 3 and 91-3, the depth of the Thule Basin is 4 km in both cases and the Moho depth differs by less than 1 km. This is an excellent agreement. Slight differences can be seen in lower crustal velocities, which are 6.3-6.6 km s⁻¹ on line 91-3 and 6.7-6.8 km s⁻¹ on Line 3. However, the signal-to-noise ratio on line 91-3 is generally not as good as on Line 3 and line 91-3 lacks P_mP reflections that can be observed over wide ranges, which were the major constraint on the lower crustal velocities on Line 3 (e.g., station 16, Fig. 4).

At its northern end, line 91-1 (Fig. 1) is less than 10 km away from line 3. There seems to be a difference of >13 km in Moho depth between the two lines (Fig. 17), which is a substantial misfit. On Line 3, Moho depth is constrained by P_mP reflections in the vicinity of the northern end of line 91-1. On line 91-1, Moho is also well constrained by P_mP reflections with exception of the northernmost 30 km of the line. In order to fit the models for the two lines, the Moho needs to shallow by 13 km from the northernmost constrained point on line 91-1 to Line 3, which is a 40 km-wide zone. This is a large change of Moho depth over such a short distance. However, the gravity map (Fig. 16) provides some support that this change is not unreasonable. The part of line 91-1 that has a Moho depth of 21 km lies within the prominent gravity high in the centre of Baffin Bay that disappears just to the south of Line 3. The maximum free-air gravity on line 91-1 is 75 mgal and decreases to -13 mgal on Line 3 where the two lines are closest. This variation in gravity can be matched by a substantial change in Moho depth, which indicates that the apparent discrepancy in crustal thickness between lines 3 and 91-1 (Fig. 17) is real. The thickness variations are probably related to the general southward thinning of the continental crust in Northern Baffin Bay as the line is approaching the continent-ocean boundary. This is also evidenced by line 91-2 that is parallel to Line 3 some 70 km to the south. Here the minimum Moho

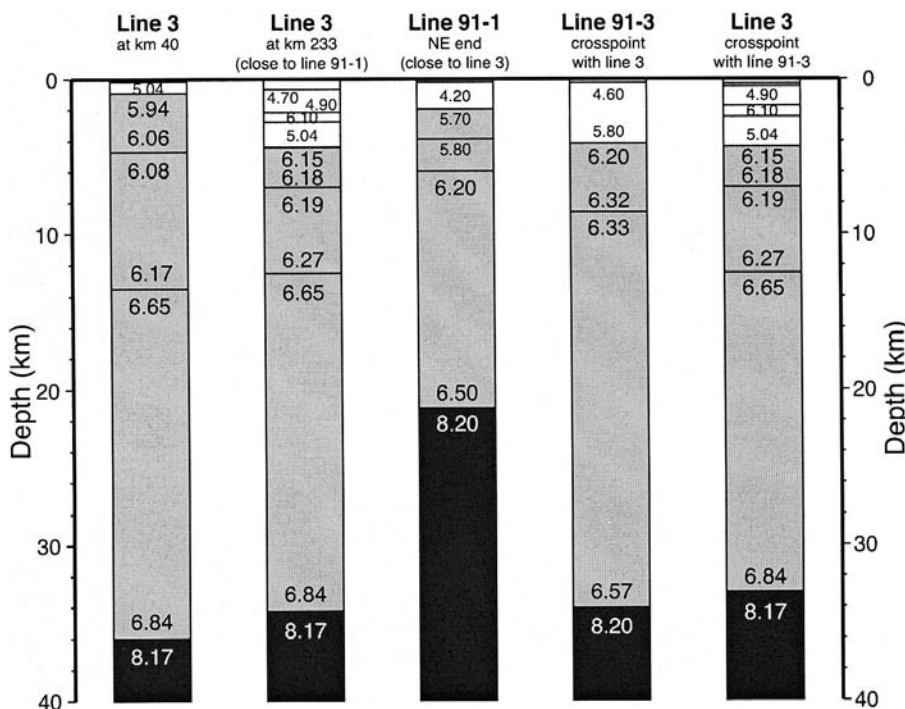


Fig. 17: Velocity-depth profiles for Line 3 and comparison with results from lines 91-1 and 91-3 (JACKSON & REID 1994). For locations see Figure 1.

depth is 17 km (REID & JACKSON 1997).

The model of line 91-1 does not show the high-velocity layer in the Thule Basin as modelled for Line 3. However, inspection of the record section of the northernmost OBS on line 91-1 (Fig. 5 in JACKSON & REID (1994)) shows evidence for a low-velocity zone (the delay occurs at an offset of 12 km) similar to the stations on Line 3 (e.g., Fig. 2). JACKSON & REID (1994) define the basement (velocity of 5.7 km s^{-1}) on line 91-1 at about the same depth level ($\sim 2.5 \text{ km}$) where we see the high-velocity layer (6.1 km s^{-1}) within the Thule Basin on Line 3 (Fig. 17). If the upper crustal layer on line 91-1 is reinterpreted as a high-velocity layer compatible to sediment layer 3, the two lines match reasonably well.

Lower crustal velocities of $6.2\text{--}6.7 \text{ km s}^{-1}$ on lines 91-1 and 91-3 (JACKSON & REID 1994) are significantly lower than those observed on Line 3 ($6.7\text{--}6.9 \text{ km s}^{-1}$; Fig. 17). We attribute this misfit to the generally lower data quality on the older lines, on which no mid-crustal reflections ($P_{c2}P$) were identified. JACKSON & REID (1994) continued therefore the rather low mid-crustal velocities down to the base of the crust. Despite the general lack of lower crustal refractions in both experiments, the lower crust on Line 3 is well resolved (Fig. 14) by numerous P_mP reflections observed over wide ranges. In contrast, resolution on lines 91-1 and 91-3 was not determined.

Other crustal scale observations from the general working area include the teleseismic receiver function analysis of DARBYSHIRE (2003). The most relevant stations in the broadband seismometer network are the ones in Pituffik/Thule Air Base (the same recorder as our station 17 on Line 3) and the station in Grise Fiord on southern Ellesmere Island (Fig. 1). Both stations are located on the Archean/Lower Proterozoic shield. The station at Grise Fiord shows the Moho as a prominent discontinuity at a depth of 34 km and the S wave velocity as 3.8 km s^{-1} below a depth of 21 km. These values compare well with Line 3, with a crustal thickness of 36 km and lower crustal S wave velocities of $3.8\text{--}3.9 \text{ km s}^{-1}$. This is an independent confirmation for the accuracy of the Poisson's ratios obtained for Line 3. The northwestern receiver functions for the station in Pituffik/Thule Air Base yield a Moho depth of 37 km and S wave velocities at a depth from 3–20 km are 3.50 km s^{-1} (DARBYSHIRE 2003). Likewise, DAHL-JENSEN et al. (2003) calculate a Moho depth of 37 km at the Pituffik/Thule Air Base station from receiver function analysis. These results also match our observations on the eastern end of Line 3 where the Moho depth is 36 km and upper and mid-crustal S wave velocities are 3.55 km s^{-1} .

CONCLUSIONS

Seismic refraction Line 3 confirms that the Proterozoic Thule Basin is an intracratonic feature that can be correlated continuously from Greenland through Nares Strait to eastern Ellesmere Island. The thickness of the basin varies between 4–5 km and the most characteristic layer within the basin is a high-velocity layer, which is probably associated with basaltic sills of the Cape Combermere Formation. Depth variations of this well-mapped layer indicate horst and graben structures within the basin.

P wave velocities, Poisson's ratios and Moho depth are almost identical on the Canadian Shield and in Greenland, indicating that both sides of Nares Strait belong to the same geological province. Absence of significant lateral changes within the crust is difficult to reconcile with interpretations that southern Nares Strait is a major plate-tectonic boundary separating Greenland from North America. However, this could still leave the possibility that strike-slip movement occurred within the Archean/Lower Proterozoic shield, which would be difficult to resolve if the crustal composition on either side of the fault is similar. If there is a strike-slip fault, the most likely horizons to detect it would be the Thule basin and the Moho, since these are well imaged. However, despite undulations in the depth of the high-velocity layer in the Thule basin (sediment layer 3) there is no indication for a sudden jump in layer depth, which could support a strike-slip fault. Similarly, the Moho stays flat at 36 km other than in the zone from km 220–320. But this Moho shallowing is associated with local uplift around the Carey Islands and there is no linear trend in the gravity data (Fig. 16) that would suggest that the crustal thinning is a linear feature as one would expect from a fault.

In consequence, if there is no obvious transform plate boundary in southern Nares Strait, eastern Ellesmere Island is possibly part of the Greenland plate and moved together with it. In this case, the plate boundary could be located on Ellesmere Island. Moho depth on line 3 is basically not resolved west of km 100 (Fig. 13), which is also the region where the crustal velocities are less resolved. Hence, there could be room in the velocity model to accommodate a plate boundary west of km 100, which is just not resolved by the sparse data in that region. More likely it should be found west of km 60 where the surface geology changes from the Archean/Proterozoic shield in the east to Paleozoic rocks of the Arctic platform in the west (Fig. 1).

ACKNOWLEDGMENTS

We thank the officers, crew, helicopter pilots, technicians, and scientists onboard CCGS "Louis S. St-Laurent" for the support in carrying out the experiment. Trine Dahl-Jensen provided the data from the broadband seismometer in Pituffik/Thule Air Base. The manuscript was improved by constructive comments by Keith Louden and Wilfried Jokat. The Nares Strait cruise was funded by the German Federal Agency of Geosciences and Natural Resources (BGR) and by the Geological Survey of Canada (GSC). Data analysis was covered by grants of the Danish National Research Foundation (Danmarks Grundforskningsfond).

References

- Bendix-Almgreen, S.E., Fristrup, B. & Nichols, R.L. (1967): Notes on the geology and geomorphology of the Carey Øer, north-west Greenland.- Meddel. om Grønland 164: 1-19.
- Christensen, N.I. & Mooney, W.D. (1995): Seismic velocity structure and composition of the continental crust: a global view.- J. Geophys. Res. 100: 9761-9788.
- Dahl-Jensen, T., Larsen, T.B., Woelbern, I., Bach, T., Hanka, W., Kind, R., Gregersen, S., Mosegaard, K., Voss, P. & Gudmundsson, O. (2003): Depth to Moho in Greenland: Receiver function analysis suggest two Proterozoic blocks in Greenland.- Earth Planet. Sci. Letters 205: 379-393.
- Darbyshire, F.A. (2003): Crustal structure across the Canadian high Arctic region from teleseismic receiver function analysis.- Geophys. J. Internat.

- 152: 372-391.
- Dawes, P.R. (1976): Precambrian to Tertiary of northern Greenland.- In: A. Escher & W.S. Watt (eds), *Geology of Greenland*, Geol. Surv. Greenland, Copenhagen, 248-303.
- Dawes, P.R. (1997): The Proterozoic Thule Supergroup, Greenland and Canada: History, lithostratigraphy and development.- *Geol. Greenland Surv. Bull.* 174: 1-150.
- Dawes, P.R. & Kerr, J.W. (1982a): Nares Strait and the drift of Greenland: a conflict in plate tectonics.- *Meddel. om Grønland, Geosci.* 8: 1-392.
- Dawes, P.R. & Kerr, J.W. (1982b): The case against major displacement along Nares Strait.- *Meddel. om Grønland, Geosci.* 8: 369-386.
- DESERT Group, Weber, M., Abu-Ayyash, K., Abueladas, A., Agnon, A., Al-Amoush, H., Babeyko, A., Bartov, Y., Baumann, M., Ben-Avraham, Z., Bock, G., Bribach, J., El-Kelani, R., Förster, A., Förster, H.J., Frieslander, U., Garfunkel, Z., Grunewald, S., Götz, H.J., Haak, V., Haberland, Ch., Hassouneh, M., Helwig, S., Hofstetter, A., Jäckel, K.-H., Kesten, D., Kind, R., Maercklin, N., Mechie, J., Mohsen, A., Neubauer, F.M., Oberhänsli, R., Qabbani, I., Ritter, O., Rümpler, G., Rybakov, M., Ryberg, T., Scherbaum, F., Schmidt, J., Schulze, A., Sobolev, S., Stiller, M., Thoss, H., Weckmann, U. & Wylegalla, K. (2004): The crustal structure of the Dead Sea Transform.- *Geophys. J. Internat.* 156: 655-681.
- Funck, T., Jackson, H.R., Reid, I.D. & Dehler, S.A. (2002): Refraction seismic studies in Nares Strait between Ellesmere Island, Nunavut, and northwest Greenland.- *Current Res.* 2002-E11: 1-6, Geol. Surv. Canada.
- Guest, W.S., Thomson, C.J., & Spencer, C.P. (1993): Anisotropic reflection and transmission calculations with application to a crustal seismic survey from the East Greenland shelf.- *J. Geophys. Res.* 98: 14161-14184.
- Harrison, J.C. (in press) Development of a new Geological map of the Nares Strait region.
- Holbrook, W.S., Mooney, W.D. & Christensen, N.I. (1992): The seismic velocity structure of the deep continental crust.- In: D.M. Fountain, R. Arculus & R. Kay (eds), *Continental lower crust*, Elsevier, Amsterdam, 1-43.
- Hood, P.J. & Bower, M. (1975): Northern Baffin Bay: Low level aeromagnetic profiles obtained in 1974.- *Report Activ., Part A. Geol. Surv. Canada, Paper 75-1A*, 89-93.
- Jackson, H.R., Dickie, K. & Marillier, F. (1992): A seismic reflection study of northern Baffin Bay: Implication for tectonic evolution.- *Can. J. Earth Sci.* 29: 2353-2369.
- Jackson, H.R. & Reid, I. (1994): Crustal thickness between the Greenland and Ellesmere Island margins determined from seismic refraction.- *Can. J. Earth Sci.* 31: 1407-1418.
- Keen, C.E. & Barrett, D.L. (1973): Structural characteristics of some sedimentary basins in northern Baffin Bay.- *Can. J. Earth Sci.* 10: 1267-1278.
- Ludwig, W.J., Nafe, J.E. & Drake, C.L. (1970): Seismic refraction.- In: A.E. Maxwell (ed), *The Sea*, Wiley Interscience, New York, 53-84.
- Lutter, W.J. & Nowack, R.L. (1990): Inversion for crustal structure using reflections from the PASSCAL Ouachita experiment.- *J. Geophys. Res.* 95: 4633-4646.
- Newman, P.H. (1982): Marine geophysical study of southern Nares Strait.- *Meddel. om Grønland, Geosci.* 8: 255-260.
- Oakey, G., Hearty, B., Forsberg, R. & Jackson, H.R. (2001): Gravity anomaly map, Bouguer on land, free air at sea, Innuitian region, Canadian and Greenland Arctic, scale 1:1500000.- *Geol. Surv. Canada, Calgary, Open file 3934D*.
- Peel, J.S. & Christie, R.L. (1982): Cambrian-Ordovician platform stratigraphy: Correlations around Kane Basin.- *Meddel. om Grønland, Geosci.* 8: 117-135.
- Reid, I. & Jackson, H.R. (1997): Crustal structure of northern Baffin Bay: Seismic refraction results and tectonic implications.- *J. Geophys. Res.* 102: 523-542.
- Roest, W.R. & Srivastava, S.P. (1989): Sea-floor spreading in the Labrador Sea: A new reconstruction.- *Geology* 17: 1000-1003.
- Ross, D.I. & Falconer, R.K.H. (1975): Geological studies of Baffin Bay, Davis Strait, and adjacent continental margins.- *Geol. Surv. Canada, Paper 75-1*: 181-183.
- Srivastava, S.P. (1985): Evolution of the Eurasian Basin and its implications to the motion of Greenland along Nares Strait.- *Tectonophysics* 114: 29-53.
- Talwani, M., Worzel, J.L. & Landisman, M. (1959): Rapid gravity computations for two-dimensional bodies with application to the Mendocino submarine fracture zone.- *J. Geophys. Res.* 64: 49-59.
- Trettin, H.P. (1991): Tectonic framework.- In: H.P. Trettin (ed), *Geology of the Innuitian Orogen and Arctic platform of Canada and Greenland*, *Geology of Canada 3*, Geol. Surv. Canada, Ottawa, 57-66.
- Williamson, M.-C. (1988): The Cretaceous igneous province of the Sverdrup Basin, Canadian Arctic: Field relations and petrochemical studies.- Ph.D. thesis, Dalhousie University, Halifax, 1-416.
- Zelt, C.A. (1999): Modelling strategies and model assessment for wide-angle seismic traveltimes data.- *Geophys. J. Internat.* 139: 183-204.
- Zelt, C.A. & Forsyth, D.A. (1994): Modeling wide-angle seismic data for crustal structure: Southeastern Grenville Province.- *J. Geophys. Res.* 99: 11687-11704.
- Zelt, C.A., & Smith, R.B. (1992): Seismic traveltimes inversion for 2-D crustal velocity structure.- *Geophys. J. Internat.* 108: 16-34.